

## EFFECT OF VOLTAGE ON TiO<sub>2</sub> NANOTUBES FORMATION IN ETHYLENE GLYCOL SOLUTION

Syahriza Ismail<sup>a\*</sup>, Khairil Azwa Khairul<sup>a</sup>, Nurul Asyikin Ahmad Nor Hisham<sup>a</sup>, Md Shuhazly Mamat<sup>b</sup>, Mohd Asyadi Azam<sup>a</sup>

<sup>a</sup>Carbon Research Technology Group, Faculty of Manufacturing Engineering, Universiti Teknikal Malaysia Melaka, Malaysia

<sup>b</sup>Department of Physics, Faculty of Science, Universiti Putra Malaysia, Selangor, Malaysia

### Article history

Received

30 August 2016

Received in revised form

13 November 2016

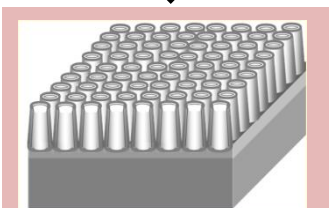
Accepted

13 March 2017

\*Corresponding author  
syahriza@utem.edu.my

### Graphical abstract

Anodization of Ti foils in ethylene glycol (EG) ammonium fluoride (NH<sub>4</sub>F), and hydrogen peroxide (H<sub>2</sub>O<sub>2</sub>) nanostructure.



Tubular structure of TiO<sub>2</sub> nanotubes form on Ti Foil.

### Abstract

The crystalline phase of the TiO<sub>2</sub> nanotubes without further heat treatment were studied. The TiO<sub>2</sub> nanotube arrays were produced by anodization of Ti foil at three different voltage; 10, 40, and 60 V in a bath with electrolytes composed of ethylene glycol (EG), ammonium fluoride (NH<sub>4</sub>F), and hydrogen peroxide (H<sub>2</sub>O<sub>2</sub>). The H<sub>2</sub>O<sub>2</sub> is a strong oxidizing agent which was used as oxygen provider to increase the oxidation rate for synthesizing highly ordered and smooth TiO<sub>2</sub> nanotubes. Anodization at voltage greater than 10 V leads to the formation of tubular structure where higher anodization voltage (~ 60 V) yield to larger tube diameter (~ 180 nm). Crystallinity of the nanotubes is improved as the voltage was increased. The transformation of amorphous to anatase can be obtained for as anodized TiO<sub>2</sub> without any heat treatment. The Raman spectra results show the anodization at 40 V and 60 V gives anatase peak in which confirms the crystalline phase. The stabilization of the crystalline phase is due to the oxygen vacancies and ionic mobilities during the anodization at high voltage.

Keywords: TiO<sub>2</sub> nanotubes, anodization, crystallization, anatase

© 2017 Penerbit UTM Press. All rights reserved

## 1.0 INTRODUCTION

TiO<sub>2</sub> is a very useful non-toxic, environmentally friendly, corrosion-resistant material. They exhibit promising performance and have been widely exploited for use in the areas of batteries development as anode materials [1], hydrogen generation [2] photocatalysts [3, 4] and many more. In many applications TiO<sub>2</sub> nanotubes is favorable than sintered TiO<sub>2</sub> nanoparticle films because, self-organized TiO<sub>2</sub> nanotube arrays provide a direct pathway for efficient electron transport rather than electrons hopping between the nanoparticles [5].

TiO<sub>2</sub> can be produced by using anodic oxidation processes. TiO<sub>2</sub> can be produced by anodization either in organic or aqueous electrolyte with various additives as the oxidation agent. The idea is that by adding additive such as water or H<sub>2</sub>O<sub>2</sub>, the rate of nanotube formation can be increase as well as

giving smooth nanotube structures [6]. As reported by Sreekantan *et al.*, the rate of formation is noted to determine the effect of electrolytes on the time required to produce nanotubes [7]. They are several influential factors in anodization such as anodizing voltage, the oxidation time, pH and concentrations of fluoride ions apart from the electrolyte mentioned. TiO<sub>2</sub> can be formed at the right potential range, which is generally called potential window [8]. When the oxidation potential is lower than the potential window, the only nonporous film is formed on the Ti film; however, when the potential is too high, a sponge oxide layer is formed [9]. The potential window generally ranges from 10 V to 40 V. The formations of TiO<sub>2</sub> nanotubes in organic solution has uniform shape and are very regular, and the extra-long tubes with smooth surface can be obtained compared with an aqueous solution.

Since the as-prepared anodic TiO<sub>2</sub> nanotube arrays are amorphous [10, 11], high temperature annealing is necessary to convert them into crystalline forms for high performance applications [12]. However, to the best of our knowledge, little work has been done on the study of amorphous to crystalline anatase TiO<sub>2</sub> formation at room temperature. Herein, we described the fabrication of TiO<sub>2</sub> nanotube arrays, from electrochemically anodized Ti foil. The TiO<sub>2</sub> pores, which were formed due to the electrochemical dissolution, induced the formation of TiO<sub>2</sub> nanotubes. The highly ordered TiO<sub>2</sub> nanotube arrays growth inwards are thus formed. The transformation of as-anodized amorphous TiO<sub>2</sub> nanotubes into the anatase phase as a function of voltage supplied was scrutinized by Raman spectroscopic measurements. The annealing process of TiO<sub>2</sub> nanotubes is included in this experiment as to provide additional information on intensification of anatase peak after heat treatment.

## 2.0 METHODOLOGY

Ti foils (99.5% purity) with 0.25 mm thickness Ti was cut into 1 cm x 3 cm to be used for anodization sample and prior to the anodization treatment, the samples were degreased by sonicating in ethanol and distilled water for 5 minutes each and dried using air gun. Finally followed by rinsing with deionized water and dried in air stream. The foils were anodized for 60 min in ethylene glycol with 5 % hydrogen peroxide (H<sub>2</sub>O<sub>2</sub>) electrolytes containing NH<sub>4</sub>F (0.3 wt%) by using two electrode configuration and a high-voltage potentiostat (Instek GPC 6030D). The purity of electrolyte of ethylene glycol is 100 %. Anodization was carried out under potentiostatic control at varied voltage of 10 V, 40 V and 60 V with graphite as cathode and Ti foil as anode. The schematic diagram of the anodization set-up is shown in Figure 1. After the anodization process, the samples were then annealed at 450 °C for 2 h in air with heating rate of 10 °C/min.

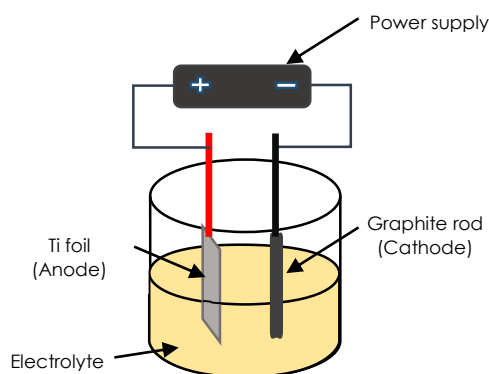


**Figure 1** Schematic diagram of the anodization set-up

The morphology and structure of TiO<sub>2</sub> nanostructure was characterized by field emission

scanning electron microscope (FESEM, Hitachi, Japan). The crystalline phase of the nanostructure was identified by x-ray diffraction (XRD) using an Analytical X'Pert Pro diffractometer with Cu K $\alpha$  radiation ( $\lambda = 0.154$  nm). Raman spectroscopy (LabRAM HR800) was used to determine the nanostructure using 532 nm laser excitation.

## 3.0 RESULTS AND DISCUSSION

### 3.1 Formation of TiO<sub>2</sub> Nanotubes

Figure 2 show the FESEM image of top view and cross sectional morphology of anodized Ti foils in ethylene glycol at three different formation voltage. Insets show the high magnification surface morphology of oxide. The evolution of morphologies for TiO<sub>2</sub> nanotubes as function of (a) 10 V, (b) 40 V, and (c) 60 V is shown in these Figures (Figure 2 (a)-(f) where the nanotubes can only be observed when the supplied voltage is 40 V.

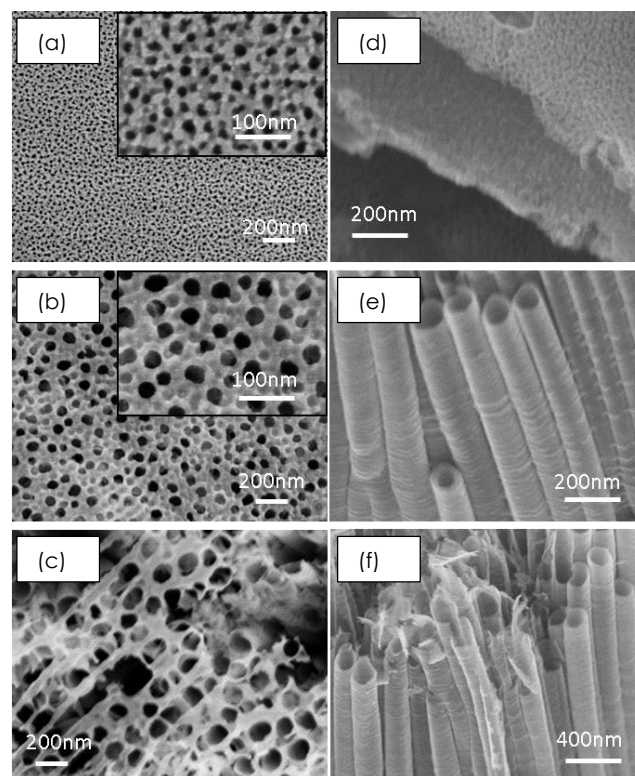


**Figure 2** FESEM images of TiO<sub>2</sub> nanotubes obtained in ethylene glycol containing NH<sub>4</sub>F and 5 % H<sub>2</sub>O<sub>2</sub> at different anodization voltages. Top surface images, (a) 10 V; (b) 40 V; and (c) 60 V. Cross section images, (d) 10 V; (e) 40 V; and (f) 60 V

At 10V, the anodic layer has porous-like top structures (Figure 2(a)). At this voltage nanotubular is hardly seen however smaller pores (~ 20 nm) can be seen on the surface of the anodic film as shown in the inset of Figure 2(a). It is because the formation of oxide layer is too thin when the anodization at 10 V. The thin layer of oxide hinder the possibility of oxide layer dissolution to form the tubes structure. As

the voltage increased to 40V pores enlargement occurred. The cross section of the Figure 2(e) indicate that the nanotubes is formed and large pores formation with diameter about 100 nm can be seen in the inset of Figure 2(b). At 60V nanotubes with larger diameter (~ 180 nm) are formed (Figure 2(c)). Nanotubular arrays are seen to have well organized and single layer oxide. Unlike samples made at 40 V, sample made at 60 V is consisted of prominent nanotubular arrays with ruptured tubes mouth. Due to the higher electric field (higher voltage), the pores formation is dominated by the electric field dissolution. Pore growth is effected by electric field. Thus, more pore formation happens, as higher field is established across the sample. It was found that higher voltage normally yielded larger tube diameter and length. Hence the stability of the structure is easily disturbed which eventually caused the rupture of the tubes mouth. The tip of the tubes is also uneven as we can see there are tubes growths underneath the perforated mouth tubes that are sitting on the formed nanotubes layer.

### 3.2 Structural Analysis

Figure 3 indicates that the XRD patterns of as anodized TiO<sub>2</sub> nanotubes at three different voltages. From the figure it is noted that only the diffraction from Ti substrate can be seen. This diffraction is caused by the thickness of TiO<sub>2</sub> nanotubes layer which is only a few nanometres. Since the penetration of the incident X-ray beam is quite high therefore, signals from the Ti substrate are very strong.

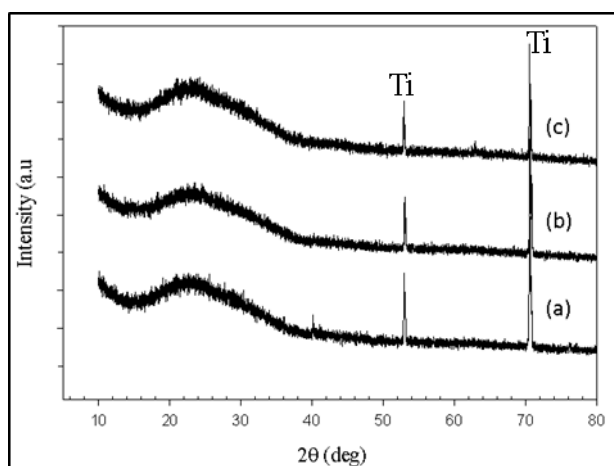


**Figure 3** XRD patterns of as anodized TiO<sub>2</sub> nanotubes obtained in ethylene glycol containing NH<sub>4</sub>F and 5 % H<sub>2</sub>O<sub>2</sub> at different anodization voltages : (a) 10 V; (b) 40 V; and (c) 60 V

Further analysis was done to ensure the phase formation of the as anodized samples in ethylene glycol solution using Raman spectroscopy. This technique allows the signals from the oxide grown on the metallic substrate to be detected. There are no Raman peaks at 10 V, indicating the presence of amorphous material. This is due to the metallic

nature of Ti that has free electrons which preventing the lattice vibrations and therefore no Raman active detected [13]. Meanwhile the spectra begin to change at 40 V and 60 V. The appearance of anatase (A) for the 40 voltage peaks at 160.1 cm<sup>-1</sup>, 264.2 cm<sup>-1</sup>, 420.6 cm<sup>-1</sup> and 620.2 cm<sup>-1</sup>. Similar peaks obtained for 60 V which is 162.3 cm<sup>-1</sup>, 209.2 cm<sup>-1</sup>, 278.0 cm<sup>-1</sup>, 420.6 cm<sup>-1</sup>, 513.0 cm<sup>-1</sup>, and 628.3 cm<sup>-1</sup> as reported in previous study [14]. Hence it can be concluded that the as anodized samples of TiO<sub>2</sub> are crystalline as proven by the Raman result in Figure 4. It is well known that anodic TiO<sub>2</sub> shows an amorphous-to-crystalline transition with anodization. This has been reported by Leach *et al.*, where crystallization results in high electronic conductivity, which enables oxygen evolution on crystalline regions to occur [15]. Thus, breakdown of anodic TiO<sub>2</sub> has been defined by oxygen evolution associated with crystallization [15]. It is possible to speculate that during the formation of oxide layer, the migration of O<sup>2-</sup> introduces high level of oxygen vacancies in the oxide. The presences of these oxygen vacancies may have promoted the formation of anatase TiO<sub>2</sub> [16]. The stabilization of the crystalline phase at room temperature can also be associated with the mobilities of various electrolyte-derived species such as fluoride ions, hydroxide ions as well as other impurities. This is reported by Habazaki *et al.* where the incorporation of species from the electrolyte into anodic titania is shown to stabilise the structure of the film [17].

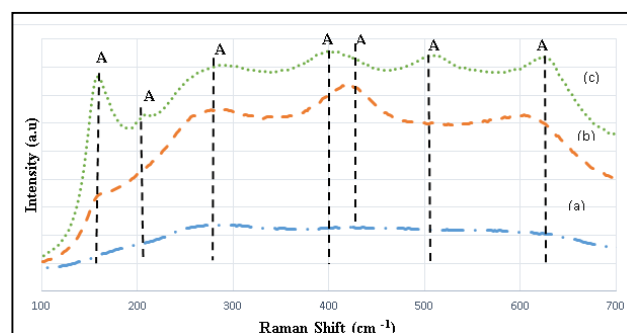


**Figure 4** Raman spectra of as anodized TiO<sub>2</sub> nanotubes obtained in ethylene glycol containing NH<sub>4</sub>F and 5 % H<sub>2</sub>O<sub>2</sub> at different anodization voltages: (a) 10 V; (b) 40 V; and (c) 60 V

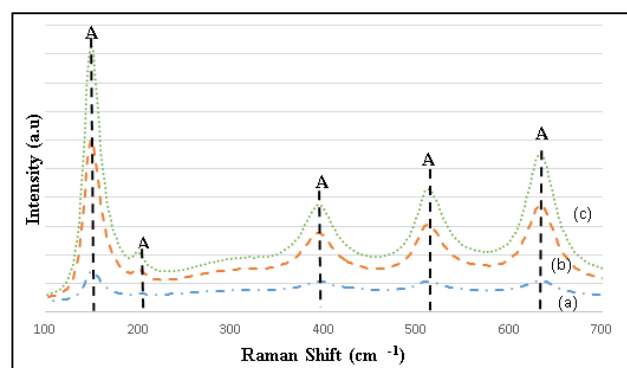


**Figure 5** Raman spectra of annealed TiO<sub>2</sub> nanotubes for samples in Figure 4 at 450°C for 2 h

After the annealing process, the intensity values for the Raman shift have been increased. An observation of the phase changes has been made, There are five Raman peaks for sample anodized at 10, 40 and 60V, indicating the presence of anatase phase. The appearance of anatase (A) for the all the samples can be seen at 160.0  $\text{cm}^{-1}$ , 199.5  $\text{cm}^{-1}$ , 393.6  $\text{cm}^{-1}$ , 513.0  $\text{cm}^{-1}$ , and 628.3  $\text{cm}^{-1}$ . The annealing has intensified the anatase peak giving out the prominent peaks as seen in Figure 5.

#### 4.0 CONCLUSION

The present work describes the influence of the anodization voltage on the structural and morphology of  $\text{TiO}_2$  nanotubes formed on Ti in ethylene glycol containing small amounts of fluoride. The morphological features of the nanotubes were related to a fluoride-induced dissolution of a porous structure. It is clear that, samples prepared at higher voltages than 10 V have crystalline anatase phase due to the transformation of as-anodized amorphous  $\text{TiO}_2$  nanotubes into the anatase structure. Hence, the crystallinity improves as the voltage was increased. The stabilization of the crystalline phase is highly dependent on the oxygen vacancies and ionic mobilities. This work has demonstrates a simple route to producing various  $\text{TiO}_2$  nanostructures that may further extend the high performance applications of semiconductor  $\text{TiO}_2$ , but also provides valuable insights into the amorphous to crystalline transformation at room temperature in anodic  $\text{TiO}_2$  nanotube.

#### Acknowledgement

The author would like to thank the Universiti Teknikal Malaysia Melaka for sponsoring this work under PJP grant (PJP/2014/FKP(4A)/S01350), and KPT for FRGS Grant (FRGS/2/2014/TK04/FKP/03/F00241).

#### References

- [1] Tang, Y., Zhang, Y., Deng, J., Wei, J., Tam, H. L., Chandran, B. K., Dong, Z., & Chen, X. 2014. Mechanical Force-Driven Growth of Elongated Bending  $\text{TiO}_2$ -Based Nanotubular Materials for Ultrafast Rechargeable Lithium Ion Batteries. *Advanced Materials*. 26(35): 6111-6118.
- [2] Liu, N., Schneider, C., Freitag, D., Hartmann, M., Venkatesan, U., Müller, J., Spiecker, E., & Schmuki, P. 2014. Black  $\text{TiO}_2$  Nanotubes: Cocatalyst-Free Open-Circuit Hydrogen Generation. *Nano Letters*. 14(6): 3309-3313.
- [3] Chen, B., Hou, J., & Lu, K. 2013. Formation Mechanism of  $\text{TiO}_2$  Nanotubes and Their Applications in Photoelectrochemical Water Splitting and Supercapacitors. *Langmuir*. 29(19): 5911-5919.
- [4] Lin, Z. A., Lu, W. C., Wu, C. Y., & Chang, K. S. 2014. Facile Fabrication and Tuning of  $\text{TiO}_2$  Nanoarchitected Morphology Using Magnetron Sputtering and Its Applications to Photocatalysis. *Ceramics International*. 40(10): 15523-15529.
- [5] Boercker, J. E., Enache-Pommer, E., & Aydil, E. S. 2008. Growth Mechanism of Titanium Dioxide Nanowires for Dye-Sensitized Solar Cells. *Nanotechnology*. 19(9): 095604.
- [6] Joseph, S., & Sagayaraj, P. 2015. A Cost Effective Approach for Developing Substrate Stable  $\text{TiO}_2$  Nanotube Arrays with Tuned Morphology: A Comprehensive Study on the Role of  $\text{H}_2\text{O}_2$  and Anodization Potential. *New Journal of Chemistry*. 39(7): 5402-5409.
- [7] Sreekantan, S., Wei, L. C., & Lockman, Z. 2011. Extremely Fast Growth Rate of  $\text{TiO}_2$  Nanotube Arrays in Electrochemical Bath Containing  $\text{H}_2\text{O}_2$ . *Journal of the Electrochemical Society*. 158(12): C397-C402.
- [8] Cai, Q., Paulose, M., Varghese, O. K., & Grimes, C. A. 2005. The Effect of Electrolyte Composition on the Fabrication of Self-Organized Titanium Oxide Nanotube Arrays by Anodic Oxidation. *Journal of Materials Research*. 20(01): 230-236.
- [9] Lockman, Z., Ismail, S., Sreekantan, S., Schmidt-Mende, L., & MacManus-Driscoll, J. L. 2009. The Rapid Growth of 3  $\mu\text{m}$  Long Titania Nanotubes by Anodization of Titanium in a Neutral Electrochemical Bath. *Nanotechnology*. 21(5): 055601.
- [10] Mor, G. K., Varghese, O. K., Paulose, M., Shankar, K., & Grimes, C. A. 2006. A Review on Highly Ordered, Vertically Oriented  $\text{TiO}_2$  Nanotube Arrays: Fabrication, Material Properties, and Solar Energy Applications. *Solar Energy Materials and Solar Cells*. 90(14): 2011-2075.
- [11] Mahajan, V. K., Misra, M., Raja, K. S., & Mohapatra, S. K. 2008. Self-Organized  $\text{TiO}_2$  Nanotubular Arrays for Photoelectrochemical Hydrogen Generation: Effect of Crystallization and Defect Structures. *Journal of Physics D: Applied Physics*. 41(12): 125307.
- [12] Fang, D., Luo, Z., Huang, K., & Lagoudas, D. C. 2011. Effect of Heat Treatment on Morphology, Crystalline Structure and Photocatalysis Properties of  $\text{TiO}_2$  Nanotubes on Ti Substrate and Freestanding Membrane. *Applied Surface Science*. 257(15): 6451-6461.
- [13] Regonini, D., Jaroenworoluck, A., Stevens, R., & Bowen, C. R. 2010. Effect of Heat Treatment on the Properties and Structure of  $\text{TiO}_2$  Nanotubes: Phase Composition and Chemical Composition. *Surface and Interface Analysis*. 42(3): 139-144.
- [14] Hardcastle, F. D. 2011. Raman Spectroscopy of Titania ( $\text{TiO}_2$ ) Nanotubular Water-Splitting Catalysts. *J Ark Acad Sci*. 65: 43-48.
- [15] Dyer, C. K., & Leach, J. S. L. 1978. Breakdown and Efficiency of Anodic Oxide Growth on Titanium. *Journal of the Electrochemical Society*. 125(7): 1032-1038.
- [16] Habazaki, H., Uozumi, M., Konno, H., Shimizu, K., Skeldon, P., & Thompson, G. E. 2003. Crystallization of Anodic Titania on Titanium and Its Alloys. *Corrosion Science*. 45(9): 2063-2073.
- [17] Matykina, E., Arrabal, R., Skeldon, P., Thompson, G. E., & Habazaki, H. 2008. Influence of Grain Orientation on Oxygen Generation in Anodic Titania. *Thin Solid Films*. 516(8): 2296-2305.